

LRP 364/88

December 1988

THE BIPOLAR MOTOR: A SIMPLE DEMONSTRATION
OF DETERMINISTIC CHAOS

M.J. BALLICO, M.L. SAWLEY and F. SKIFF

THE BIPOLAR MOTOR: A SIMPLE DEMONSTRATION OF DETERMINISTIC CHAOS

M.J. Ballico, M.L. Sawley,⁺

School of Physics, The University of Sydney, N.S.W. 2006, Australia

and F. Skiff^{*}

Centre de Recherches en Physique des Plasmas,

Association Euratom - Confédération Suisse, Ecole Polytechnique Fédérale de Lausanne,

21 Avenue des Bains, 1007 Lausanne, Switzerland

Abstract

A simple and inexpensive mechanical model for the demonstration of chaos in a nonlinear deterministic system is described. Periodic, period-doubled, and chaotic motions are exhibited by the model in agreement with the solutions of its governing differential equation. The model is sufficiently free from long term drifts to enable experimental Poincaré plots to be easily constructed. Such a simple mechanical model is shown to be ideal for use as a lecture room demonstration, as well as for a student laboratory.

⁺ Present address: I.M.H.E.F., ME - Ecublens, 1015 Lausanne, Switzerland

^{*} Present address: L.P.R., University of Maryland, College Park MD 20742, U.S.A.

1. INTRODUCTION

In recent years there has been an explosive growth in the study of the chaotic behavior of nonlinear dynamical systems.^{1,2} Many applications of this work have been made across a very broad range of scientific disciplines, from electronics to ecology, meteorology to biology. Chaos generally refers to the irregular, or nonperiodic, behavior that arises from the nonlinear nature of the system. It has been found that chaos is not restricted to dynamical systems with a large number of degrees of freedom; in fact a deterministic, but nonlinear, system with only three degrees of freedom may exhibit chaotic behavior.

To demonstrate the basic features of chaotic behavior to newcomers to this field, be they teaching staff or students, there is a need for simple experimental systems that exhibit chaotic motion. Many experiments have been devised (see Ref. 1 - 5 for a review) that demonstrate various aspects of deterministic chaos. From a pedagogical viewpoint, mechanical systems that are simple to construct and easily visualized offer obvious advantages. Examples of mechanical systems that have been studied include the nonlinear pendulum,⁶ the bouncing ball,⁷ and the buckled beam.⁸ Also mentioned has been the bipolar motor, consisting of a permanent magnet rotating in an oscillating magnetic field.^{5,9-11}

In this paper we describe in detail results obtained from our model of a bipolar motor. These demonstrate clearly the advantages of such a simple mechanical system to introduce the basic concepts of deterministic chaos. Using a standard overhead projector, it is shown possible to visualize the motion of the system, both periodic and chaotic, in the lecture room. In addition, simple diagnostic techniques are described that enable measurements to be undertaken in the teaching laboratory. It is shown to be straightforward to construct experimental phase space plots that provide an essential means of viewing the behavior of a chaotic system.

2. THEORY

The equation of motion for a dipole magnet in a linearly polarized magnetic field oscillating at frequency ω is

$$\ddot{\theta} + \gamma \dot{\theta} + f \sin \theta \cos \omega t = 0, \quad (1)$$

where θ is the angle between the dipole moment and the magnetic field polarization. In Eq. (1) it has been assumed that the damping is proportional to the angular velocity of the magnet, with a damping coefficient γ . The amplitude of the driving torque is $f = \mu B_\omega / I$, where μ and I are, respectively, the magnetic dipole moment and the moment of inertia of the magnet, and B_ω is the amplitude of the oscillating magnetic field.

Equation (1) is a second order differential equation that is nonlinear due to the presence of the $\sin\theta$ term. It can be solved by standard numerical techniques to yield the motion $\theta(t)$ of the magnet for given initial conditions $\theta(0), \dot{\theta}(0)$. A study of the solutions of this equation¹¹ for a range of parameters (f, γ, ω) shows that, after the decay of transients, there exists two different types of motion. One is a regular motion that is periodic with time. An example of this type of motion occurs when the magnet rotates synchronously with the imposed oscillating field, as is commonly expected for such a motor. However, parameter values also exist for which the motion of the magnet is irregular, or chaotic. It can be shown¹¹ that upon fixing the values of γ and ω , bands of values of f exist for which the solutions of Eq. (1) are periodic, separated by bands of chaotic motion. In the first of the periodic bands, the magnet exhibits rotational motion, in the second, vibrational motion. In general, in the n^{th} periodic band the motion is rotational if n is odd and vibrational if n is even. A study of the transition from a band of periodic motion to a band of chaotic motion shows that the bipolar motor undergoes a period-doubling route to chaos.^{10,11}

With increasing values of f , the motion changes from one with a period of $T = 2\pi/\omega$, to period-doubled ($2T$), to period-quadrupled ($4T$), continuing until the motion is chaotic.

3. EXPERIMENT

The behavior described by the solutions of Eq. (1) can be experimentally observed from a simple model of the bipolar motor. Our model (see Fig. 1) was constructed using a small magnet consisting of a ferrite cylinder of diameter 27 mm and thickness 10 mm, with a magnetic dipole moment $\mu = 1.1 \text{ m}^2$ directed normal to its flat surface. The magnet was suspended in a linearly polarized magnetic field ($B_\omega \leq 4.5 \text{ mT}$) produced by passing an oscillating current (amplitude $\leq 2.1 \text{ A}$) through a pair of Helmholtz coils. The magnet was restricted to rotate about an axis perpendicular to its magnetic axis by a pair of bearings, one a roller bearing the other a point. Its moment of inertia about the axis was $I = 2.5 \times 10^{-6} \text{ kg m}^2$. The damping of the motion of the magnet was adjusted by packing the roller bearing with silicon grease. The coefficient of damping, measured by analyzing the unforced motion of the magnet after an initial impulse, was $\gamma = 0.9 \text{ s}^{-1}$. For the measurements described here, the frequency of the oscillating field was fixed at $\omega/2\pi = 2 \text{ Hz}$. The strength of the field was varied by adjusting the amplitude of the oscillating current passing through the Helmholtz coils.

Our model of the bipolar motor was constructed with the magnet and Helmholtz coils supported by a perspex (lucite) frame, enabling a clear view of the motion of the magnet. In particular, it allowed the motion to be observed on a screen by means of a standard overhead projector, providing a simple and clear lecture room demonstration.

The motion of the magnet in the oscillating field was measured using probes located nearby which detected the change in the local magnetic field. A Hall probe with its axis perpendicular to the direction of the oscillating field gave a measure of the position of the magnet $\sim \sin\theta$. Another

Hall probe was located at an angular displacement of 90° . By subtracting from its signal the contribution due to the oscillating field produced by the Helmholtz coils, a measure of the position of the magnet $\sim \cos\theta$ was obtained. A small multi-turn coil located at an angular position 180° from the first Hall probe provided a measure of the velocity of the magnet $\sim \cos\theta \dot{\theta}$. (Recording the three signals enabled, in principle, the position $\theta(t)$ and the velocity $\dot{\theta}(t)$ of the magnet to be calculated. In this paper, however, only the direct signals are presented for sake of simplicity.) Data from the probes was digitized into records of 8192 samples, generally using a sampling frequency of 500 Hz. A CAMAC-based transient digitizer (LeCroy model 2264) was used, although a storage oscilloscope would also have been suitable for recording the data. Alternatively, analogical analysis of the signals could be undertaken, as is discussed in the Appendix.

As an experimental model of Eq. (1), it should be noted that the magnet used in the bipolar motor was not a perfect dipole but contained higher order magnetic moments, and the magnetic field produced by the Helmholtz coils was not perfectly uniform. Consequently, the torque exerted on the magnet by the oscillating field was not given by $f \sin\theta \cos\omega t$, but also contained higher order angular terms. The effect of the higher order moments was also detected in the position and velocity measurements if the probes were placed too close to the magnet. In addition, there was a non-negligible static friction associated with the bearings. Thus the damping may not be accurately described solely by a velocity dependent term. The earth's magnetic field had only a small influence on the motion of the magnet: no effort was made to minimize this interaction. Despite the above discrepancies, however, the experimental model of the bipolar motor was found to exhibit both the qualitative and quantitative features observed in the solutions of Eq. (1).

4. RESULTS

Data was taken from the experimental system for a range of values of the amplitude of the oscillating current in the Helmholtz coils. Figure 2 shows, for a selection of these values, the temporal variation of the signal $\sim \sin\theta$ measured by the Hall probe after the decay of transients. The normalized amplitude of the driving torque, $F \equiv f/\omega^2$, is proportional to the amplitude of the oscillating current. F is half the ratio of the maximum potential energy of the magnet in the oscillating magnetic field to its kinetic energy when rotating synchronously with the field.

Figure 2 shows the "band structure" in the values of F exhibited by the motion of the magnet. For low values of F (e.g., $F = 0.8$), the motion was periodic, while setting $F = 1.9$, for example, rendered the motion chaotic. A further periodic band was observed for $3.6 \lesssim F \lesssim 6.8$, followed by a band of chaos. For the highest value of F achievable by our experimental system ($F = 11.9$), the motion was again periodic. For $F = 1.7$, the magnet exhibited period-doubled motion, that is, the period of the motion was twice that of the driving torque. The above observations are in quantitative agreement with theoretical predictions based on the solutions of Eq. (1).¹²

The motion of the magnet can also be displayed by its representation as a trajectory in phase space. Such plots in $(\sin\theta, \cos\theta \dot{\theta})$ space are shown in Fig. 3 for six values of F . For $F = 0.8$ (in the first periodic band), the motion is represented by a single loop, corresponding to rotation at the driving frequency. For $F = 6.3$ (in the second periodic band), the phase space plot consists of two loops, corresponding to a vibratory motion. For $F = 11.9$ (in the third periodic band), three loops in phase space are undertaken during one cycle of the driving torque, corresponding to rotation at the driving frequency with a superimposed vibration. For the period-doubled motion observed when $F = 1.7$, three loops are observed in one period of the motion, or every two periods of the driving torque. For $F = 1.9$ and 8.7 , the trajectory in phase space is non-periodic, corresponding to chaotic motion of the magnet.

Another instructive method of displaying the motion of the magnet is by means of a Poincaré section of the three dimensional phase space. This is constructed by plotting $(\sin\theta, \cos\theta, \dot{\theta})$ at the same time each period of the driving torque. In such a representation, periodic motion at the same frequency as the driving torque is exhibited as a single point and period-doubled motion as two points. More complex motion, in particular chaotic behavior, results in a more intricate Poincaré plot. Figure 4 shows examples of such plots constructed using data from the experimental bipolar motor. (These data were recorded, as required, using a sampling frequency equal to the driving frequency. The total time required to record the data for each value of F was greater than one hour.) Representations of periodic, period-doubled and chaotic motions are clearly observed. A Poincaré plot is a convenient and illustrative means of viewing the strange attractor associated with chaotic motion.^{1,2} Figures 2 - 4 demonstrate that although the temporal behavior of chaotic motion may appear random, the corresponding Poincaré plots exhibit a regular pattern. This is associated with the fact that the strange attractor does not occupy the entire phase space, but has a fractal dimension less than that of the phase space. (For the bipolar motor, the dimensions of the strange attractors are between 2 and 3.) A more detailed description of the calculation of the fractal dimension can be found in Refs. 1,2 and 11. It is important to note that despite the simple mechanical construction of our experimental bipolar motor, the motion exhibited by the magnet was stable over a very long time (> one hour). This enabled the possibility to construct the Poincaré plots shown in Fig. 4.

5. CONCLUSIONS

In this paper the bipolar motor has been proposed as a simple and inexpensive model for the demonstration and study of deterministic chaos. Periodic, period-doubled, and chaotic motions are readily observed with such a model. Phase space representations and Poincaré plots have been shown to be easily obtained, thus elucidating features of the motion not easily observed

in the raw probe signals. It has been shown possible to undertake successful qualitative and quantitative comparison with theoretical predictions. Such a model provides a very visual and appreciated lecture room demonstration, as has been evidenced by the authors on several occasions. In addition, it should find ready application in the student laboratory as an experimental demonstration of deterministic chaos.

ACKNOWLEDGMENTS

The authors wish to thank P. Denniss for constructing the amplifier used to supply the oscillating current to the Helmholtz coils. This work was partly supported by the Fonds National Suisse pour la Recherche Scientifique.

APPENDIX

Although digital acquisition and processing of experimental data are continually becoming less expensive and more convenient, analogical signal treatment may often be accomplished by simple means and may be preferred depending on the available laboratory equipment. Here we shall briefly consider analog techniques that provide the Fourier spectrum and phase-space representation of signals that are useful in the analysis of the chaotic behavior of an experimental system.

A simple audio-frequency spectrum analyser can be easily constructed, if a commercial spectrum analyser is not available. A block diagram is shown in Fig. 5(a). The low pass filter may readily be made using an operational amplifier. The analog multiplier is available as an integrated circuit¹³ and the sine wave local oscillator may be easily assembled. The signal component at the local oscillator frequency is detected by mixing to provide a d.c. signal, the bandwidth being determined both by the low pass filter and by how quickly the oscillator is swept ($1/f^2 df/dt$). Although the main spectral features of a signal are easily observed with such a set-up, ideally another multiplier should be employed to detect the signal component that is in phase quadrature with the local oscillator. The absolute value of the Fourier components can then be obtained by adding the magnitudes of the in-phase and quadrature signals.

If an oscilloscope with an analog "z-axis" (intensity) input is available, the Poincaré plot of a signal can be displayed. Figure 5(b) shows the experimental set-up. The measured "coordinates", $\sin\theta$ and $\cos\theta \dot{\theta}$, are applied to the x and y inputs of the oscilloscope yielding, after a sufficient length of time, the analog equivalent of the phase space plots shown in Fig. 3. If a series of short pulses provided by a free-running oscillator is supplied to the z input (each pulse being sufficiently long so as to produce a bright spot on the screen), the distance between points gives an indication of the passage of time along the orbit. If the oscillator is synchronized to the

generator which drives the oscillating current through the Helmholtz coils of the motor, then a Poincaré plot is obtained.

References

- 1 P. Bergé, Y. Pomeau, and Ch. Vidal, "Order within chaos" (Wiley, New York, 1986).
- 2 H.G. Schuster, "Deterministic chaos: an introduction" (2nd edition, VCH Verlag., Weinheim, 1988).
- 3 H.L. Swinney, *Physica* **7D**, 3 (1983).
- 4 N.B. Abraham, J.P. Gollub, and H.L. Swinney, *Physica* **11D**, 252 (1984).
- 5 K. Briggs, *Am. J. Phys.* **55**, 1083 (1987).
- 6 D. D'Humières, M.R. Beasley, B.A. Humberman, and A. Libchaber, *Phys. Rev. A* **26**, 3483 (1982).
- 7 N.B. Tufillaro and A.M. Albano, *Am. J. Phys.* **54**, 939 (1986); and T.M. Mello and N.B. Tufillaro, *Am. J. Phys.* **55**, 316 (1987).
- 8 F.C. Moon and W.T. Holmes, *Phys. Lett.* **111A**, 157 (1985).
- 9 V. Croquette and C. Poitou, *J. Physique - Lett.* **42**, 537 (1981).
- 10 H. Meissner and G. Schmidt, *Am. J. Phys.* **54**, 800 (1986).
- 11 C.W. Simm, M.L. Sawley, F. Skiff, and A. Pochelon, *Helv. Phys. Acta* **60**, 510 (1987).
- 12 M.L. Sawley, W. Simm, F. Skiff, and A. Pochelon, *Helv. Phys. Acta* **59**, 1070 (1986).

13 For example, Analog Devices integrated multiplier AD534.

Figure Captions

- Fig. 1. Schematic diagram of the bipolar motor. The Hall probe measuring a signal $\sim \cos\theta$ is shown, however the other two probes have not been included in the diagram for sake of clarity.
- Fig. 2. Temporal variation of the oscillating current I_ω in the Helmholtz coils, and the signals $\sim \sin\theta$ measured by a Hall probe for the indicated values of the normalized amplitude of the driving torque F .
- Fig. 3. Trajectories in phase space measured for the six indicated values of the normalized amplitude of the driving torque F .
- Fig. 4. Poincaré plots measured for the six indicated values of the normalized amplitude of the driving torque F .
- Fig. 5. Block diagrams for the analog determination of (a) the Fourier spectrum, and (b) the phase space representation of experimental signals.

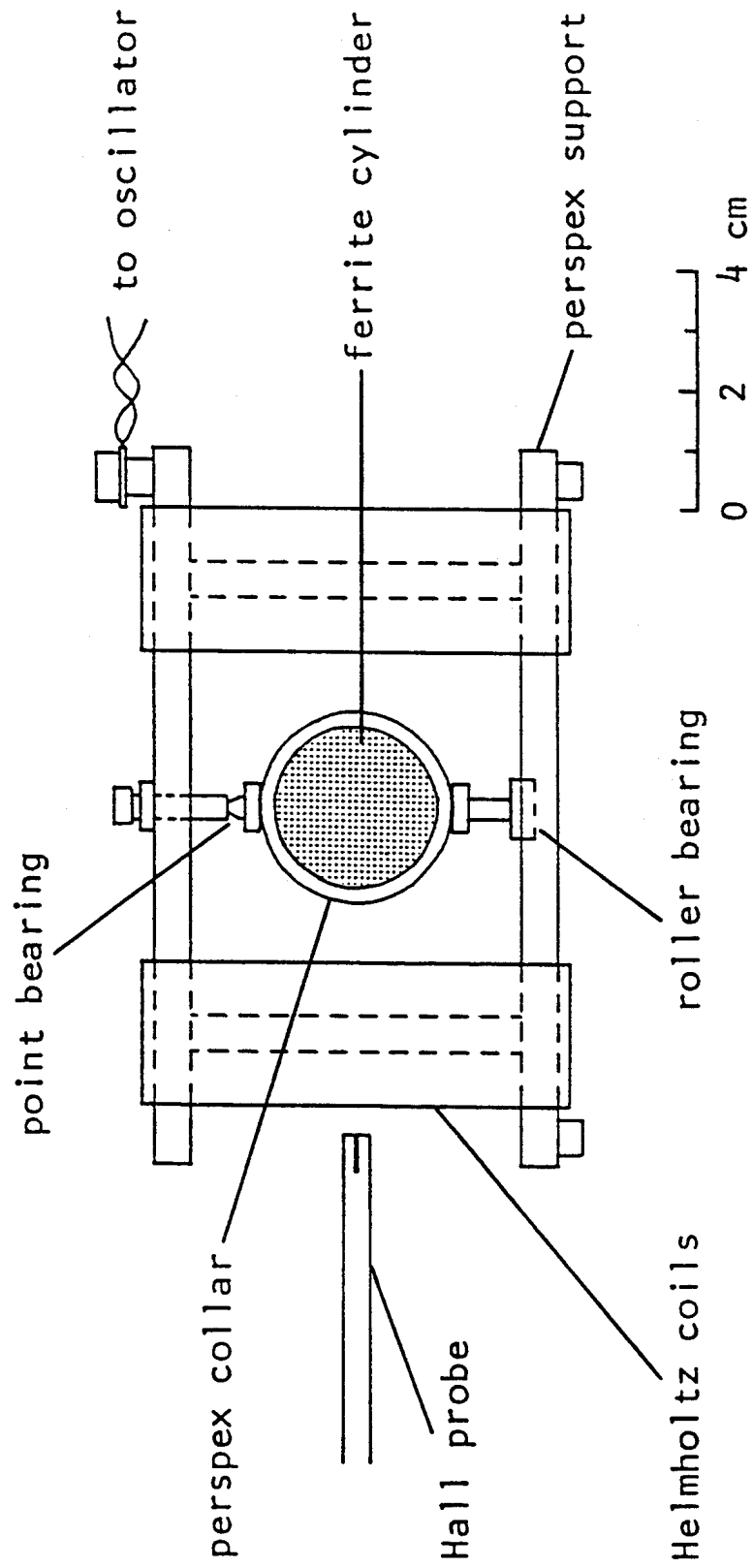


Figure 1

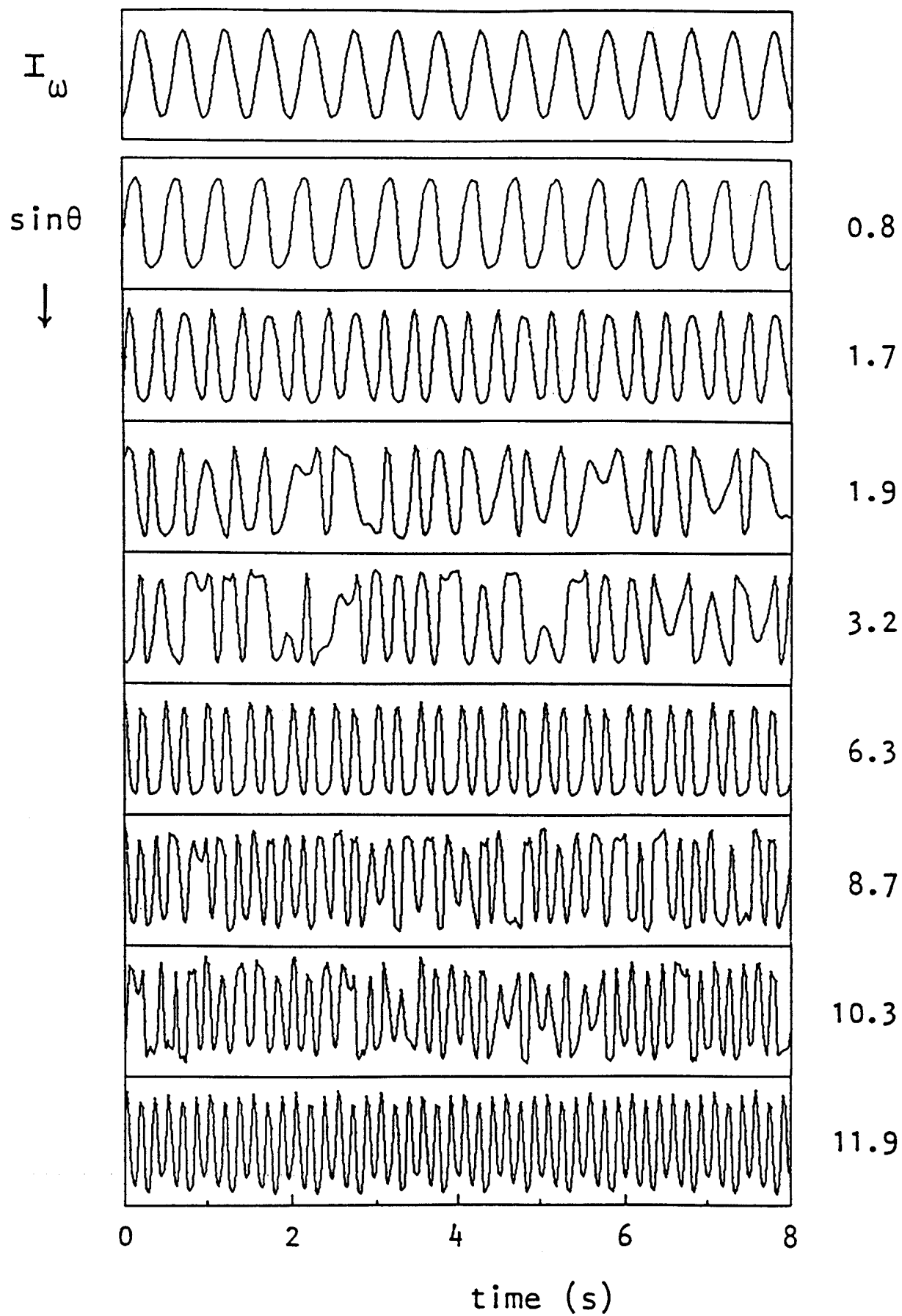
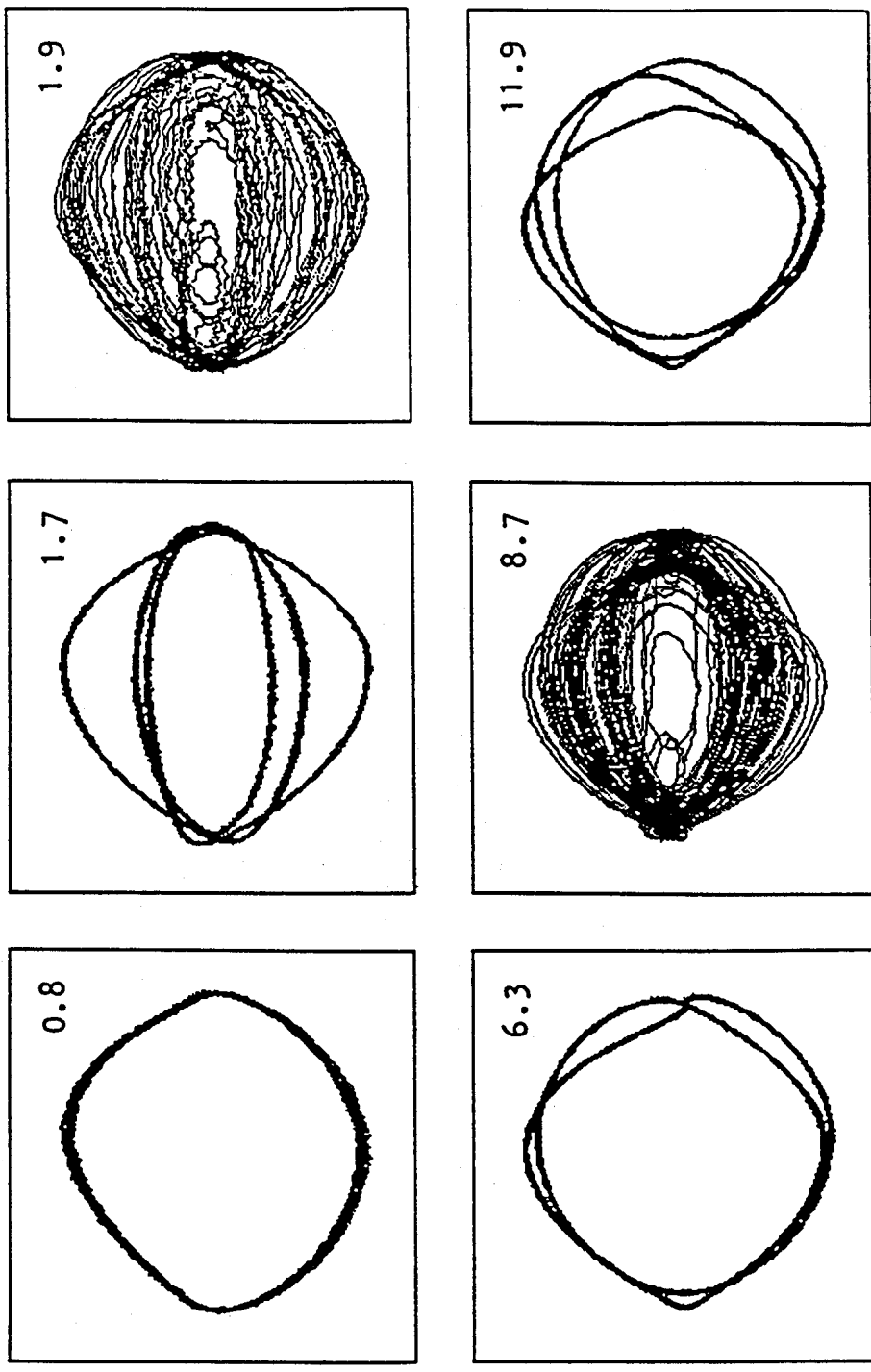


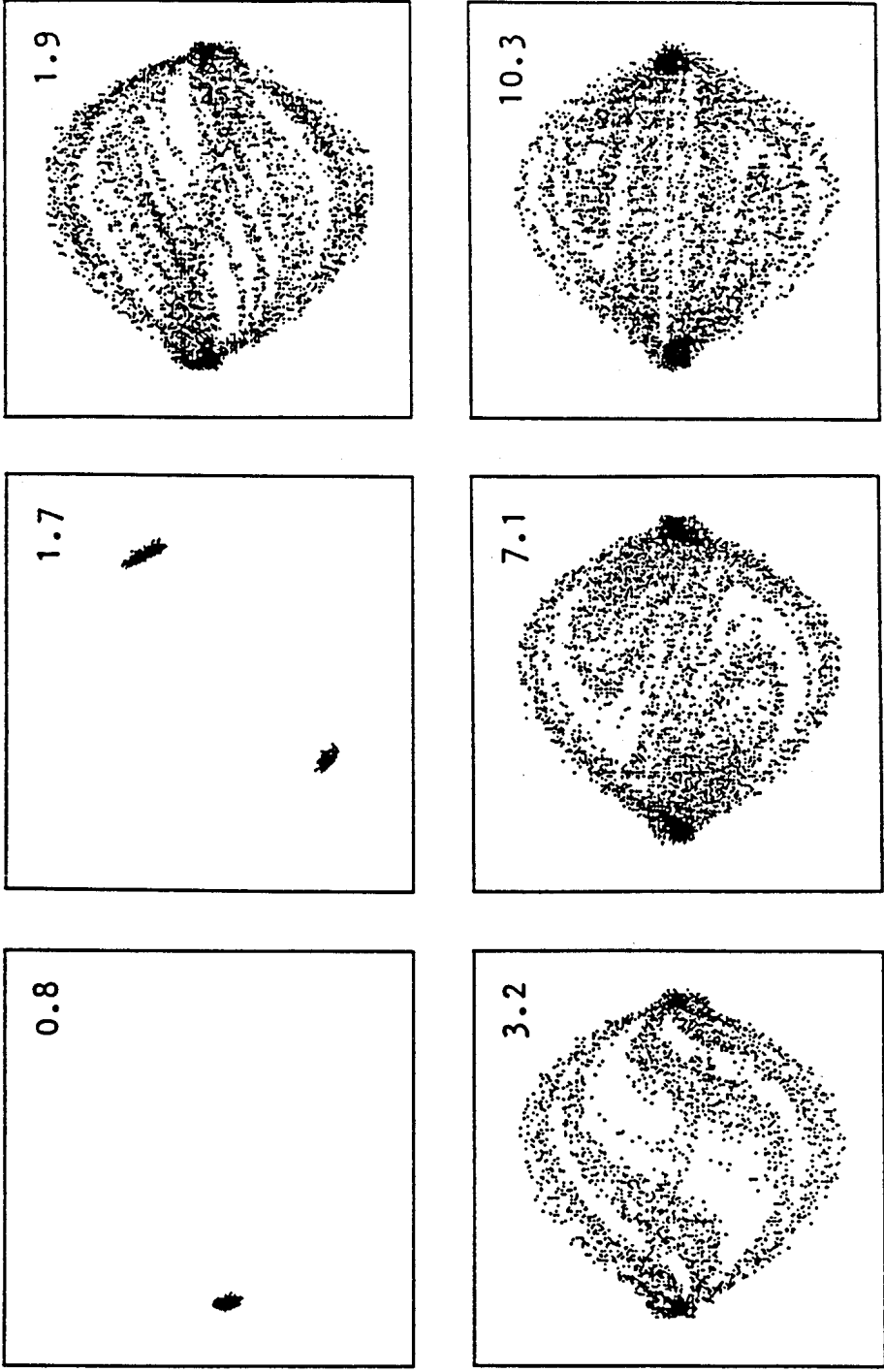
Figure 2



↑ $\cos \theta$

$\sin \theta$ →

Figure 3

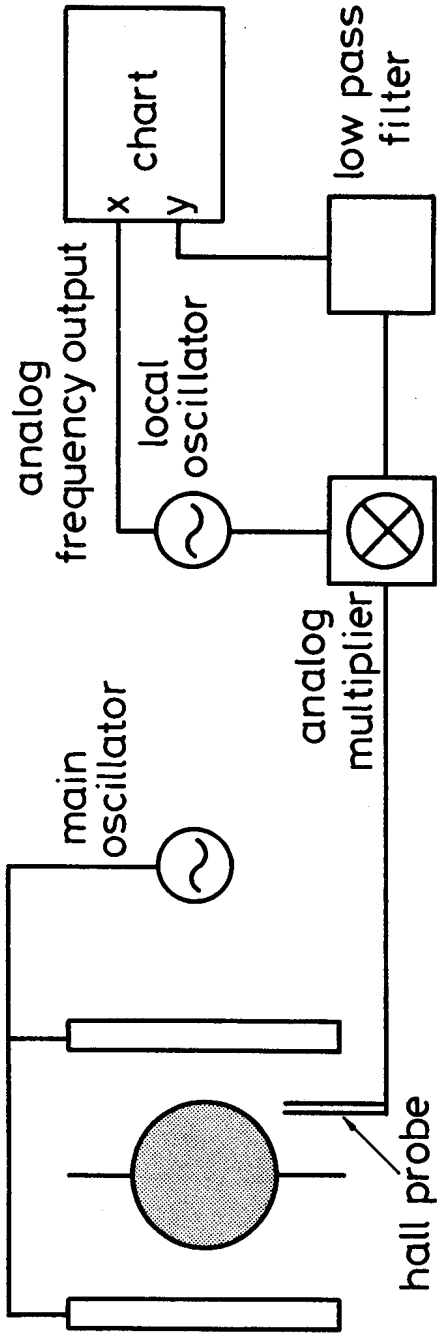


↑ $\cos \theta$

$\sin \theta$ →

Figure 4

(a)



(b)

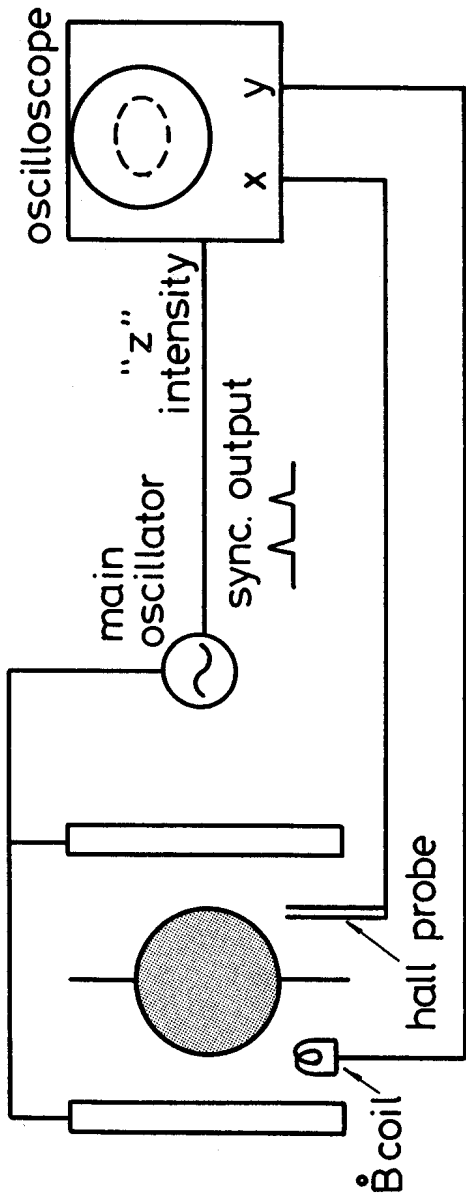


Figure 5